Characteristics of stratospheric warming events during Northern winter

Pauline Maury, Chantal Claud, Elisa Manzini, Alain Hauchecorne, Philippe Keckhut

AGU PUBLICATIONS

JGR

Journal of Geophysical Research: Atmospheres

RESEARCH ARTICLE
10.1002/2015JD024226

Key Points:
- Characterization of stratospheric warming events during wintertime
- Stratospheric warming continuum
- Polar stratospheric variability analysis

Correspondence to:
P. Maury,
pmaury@lmd.ens.fr

Citation:
Maury, P., C. Claud, E. Manzini, A. Hauchecorne, and P. Keckhut (2016), Characteristics of stratospheric warming events during Northern winter, *J. Geophys. Res. Atmos.*, *121*, 5368–5380, doi:10.1002/2015JD024226.

Received 14 SEP 2015
Accepted 22 APR 2016
Accepted article online 28 APR 2016
Published online 21 MAY 2016

Characteristics of stratospheric warming events during Northern winter

Pauline Maury[1,2], Chantal Claud[1], Elisa Manzini[3], Alain Hauchecorne[2], and Philippe Keckhut[2]

[1] Laboratoire de Météorologie Dynamique, IPSL, Ecole Polytechnique, Palaiseau, France, [2] Laboratoire Atmospheres, Milieux, Observations Spatiales, IPSL, UVSQ, CNRS-INSU, Guyancourt, France, [3] Max Planck Institute for Meteorology, Hamburg, Germany

Abstract The strong interest in Sudden Stratospheric Warmings (SSWs) is motivated by their role in the two-way stratospheric-tropospheric dynamical coupling. While most studies only investigate major SSWs (vortex breakdown), the minor ones (strong vortex deceleration) are overlooked. This work aims at overcoming this gap by providing a comprehensive description of stratospheric warming events without a priori distinctions between major and minor SSWs, leading to a more complete estimate of the stratospheric variability. Warming events are extracted from reanalysis data sets by means of a midstratospheric polar cap temperature daily index. Events are characterized by a bimodal distribution in amplitude, with a broad peak at small amplitudes (inferior to 5*K*) and a sharp peak at around 9*K*. Due to the intrinsic polar vortex dynamics, the warming amplitude presents a distinct seasonal distribution. Small amplitude warmings mainly occur during early and late wintertime by contrast with the larger-amplitude ones occurring during midwintertime. From mid-November to mid-March, the large-amplitude warmings (i.e., strong warming events, SWEs) include both major and minor SSWs, as well as Canadian and Final warmings. Although major SSWs belong to the tail of the SWEs distribution, there is no clear distinction between the major and minor SSWs according to the considered properties of the events. Such result brings out the idea of "warming continuum." Furthermore, diagnostics of heat flux reveal that there is no statistical difference between SWEs with regard to their feedbacks on the planetary waves and hence on their potential influence into the troposphere.

1. Introduction

Due to the polar night in wintertime, the high-latitude midstratosphere is characterized by westerly winds around the pole: the so-called polar vortex. The polar vortex is one of the most variable features of the zonal mean circulation of the Earth's atmosphere, which results from a nonlinear interaction between planetary-scale Rossby waves and the zonal flow [*Charney and Drazin*, 1961; *Matsuno*, 1971]. In a span of a few days, this wave mean-flow interaction leads to a zonal flow weakening and a temperature rising over the polar cap by more than 40*K* in extreme cases [*Scherhag*, 1952; *Labitzke*, 1977]. Such phenomena are known as Sudden Stratospheric Warmings (SSWs) and constitute, since their discovery in 1952 [*Scherhag*, 1952], the most impressive dynamical event in the physical climate system. SSWs are commonly defined by the reversal of the meridional temperature gradient, and the differentiation between major and minor SSWs is made according to the reversal of the westerly stratospheric polar flow at 60°N and 10 hPa (*McInturff* [1978], *Andrews et al.* [1987], and *Butler et al.* [2015], for a recent discussion on SSW definitions). Because major SSWs play an important role in the two-way stratospheric-tropospheric dynamical coupling, many studies have focused almost exclusively on them [e.g., *Charlton and Polvani*, 2007; *Gerber et al.*, 2009; *Cohen and Jones*, 2011].

However, to understand the response of the stratosphere to external tropospheric forcing and to better characterize the role of the stratosphere in pathways of climate variability, focusing solely on the extreme SSWs may be insufficient. Indeed, the mean stratospheric response during Northern wintertime to global warming is not necessarily directly related to changes in major SSW frequency [*Karpechko and Manzini*, 2012]. A comprehensive estimate of the variability of the wintertime stratosphere, including nonextreme cases, is needed to understand such mean stratospheric changes. Few studies (*Limpasuvan et al.* [2004], among others) suggest that minor SSWs can also have a tropospheric signature, justifying the examination of minor SSWs

as well. Moreover, *Coughlin and Gray* [2009] have shown that minor and major SSWs belong to a continuum of stratospheric warmings, without a well-defined threshold between both SSW types. Such studies raise the question whether considering major and minor SSWs as distinct events makes sense.

In this context, this work aims at (i) reducing the gap in the knowledge of nonextreme stratospheric variability, by using less restrictive event definitions and (ii) addressing the question of how distinct are major and minor SSWs. To achieve these aims, we provide a comprehensive description of the stratospheric warming events occurring during 54 Northern Hemisphere consecutive winters from 1959 to 2013 without any distinction between major and minor SSWs. The stratospheric temperature anomalies tend to propagate downward, and it has been shown that an empirical orthogonal function (EOF) analysis of the polar cap-averaged temperature is well adapted to capture the variability of the stratospheric polar vortex and to study its vertical structure [*Kodera et al.*, 2000; *Kuroda and Kodera*, 2004; *Zhou et al.*, 2002; *Hitchcock et al.*, 2013; *Hitchcock and Shepherd*, 2013]. The originality of the present study lies in considering only positive anomalies of a daily polar cap vertically (50–10 hPa) averaged temperature greater than 1 standard deviation from smoothed climatological mean. By construction our method allows to select events corresponding to a warm middle stratosphere, corresponding to the second temperature EOF in the study of *Hitchcock et al.* [2013] [see *Hitchcock et al.*, 2013, Figures 2 and 3]. This paper thoroughly documents and examines the global statistics of the warm events in terms of amplitude and duration and discuss their associated dynamical properties.

The paper is organized as follows: The data set and method used are introduced in section 2. Section 3 presents general statistics of stratospheric warm events. It will be shown that stratospheric warm anomalies occurring during the winter can be divided into two populations with regard to their amplitude. Thus, section 4 focuses on the stronger warm anomalies and gives a comprehensive comparison between the aforementioned warm anomalies and well-known climatologies of SSWs. Finally, a summary and a conclusion are provided in section 5.

2. Data and Method

We evaluate the properties of stratospheric warmings for the period from the beginning of October to the end of April, hereafter defined as "winter." To extend the range of years investigated, two reanalysis products from the European Centre for Medium-Range Weather Forecasts (ECMWF), have been used. The first set considers daily data over 20 years from ERA-40 [*Uppala et al.*, 2005], from 1 October 1959 to 30 April 1979. The second one considers daily data over 34 years from ERA-Interim (ERA-I) [*Dee et al.*, 2011], from 1 October 1979 to 30 April 2013. Considering that ERA-40 data sets are available until 2002, a Student's *t* test has been used to check that both reanalysis products do not statistically differ in terms of mean and variability during the wintertime for the 20 overlapping years. In this way, 54 consecutive winters are used, spanning from 1959 to 2013, and the resulting merged product is noted ERA in the following.

2.1. Stratospheric Polar Cap Temperature Index

Stratospheric warming events are extracted from the ERA temperature daily time series by means of a midstratospheric polar cap temperature anomaly index.

1. For each year, a stratospheric polar cap temperature is computed from the daily zonal mean temperature by averaging (i) latitudinally, the cosine-weighted temperature between 70°N and 90°N, and (ii) vertically, the pressure-weighted mean between 50 hPa and 10 hPa. This daily field is noted $T(t_{d,y})$, where T refers to the temperature and t to the time with the subscripts d and y denoting the day and the year, respectively.
2. For each year, a 21 day running window is applied on the daily values $T(t_{d,y})$ to remove high-frequency variations. From the resulting filtered field (hereafter, low-frequency)—noted $T_{21d}(t_{d,y})$—the mean $\mathcal{M}_{T_{21d}}(t_d)$ and the standard deviation $\sigma_{T_{21d}}(t_d)$ are calculated. The low-frequency mean $\mathcal{M}_{T_{21d}}(t_d)$ is represented in Figure 1a, together with its deviation by $\pm 1\sigma_{T_{21d}}(t_d)$.
3. The index $\mathcal{I}_T(t_{d,y})$ of midstratospheric polar cap temperature anomalies are eventually defined as the unfiltered daily temperature deviation from the low-frequency mean, normalized by the low-frequency standard deviation:

$$\mathcal{I}_T(t_{d,y}) = \frac{T(t_{d,y}) - \mathcal{M}_{T_{21d}}(t_d)}{\sigma_{T_{21d}}(t_d)}. \quad (1)$$

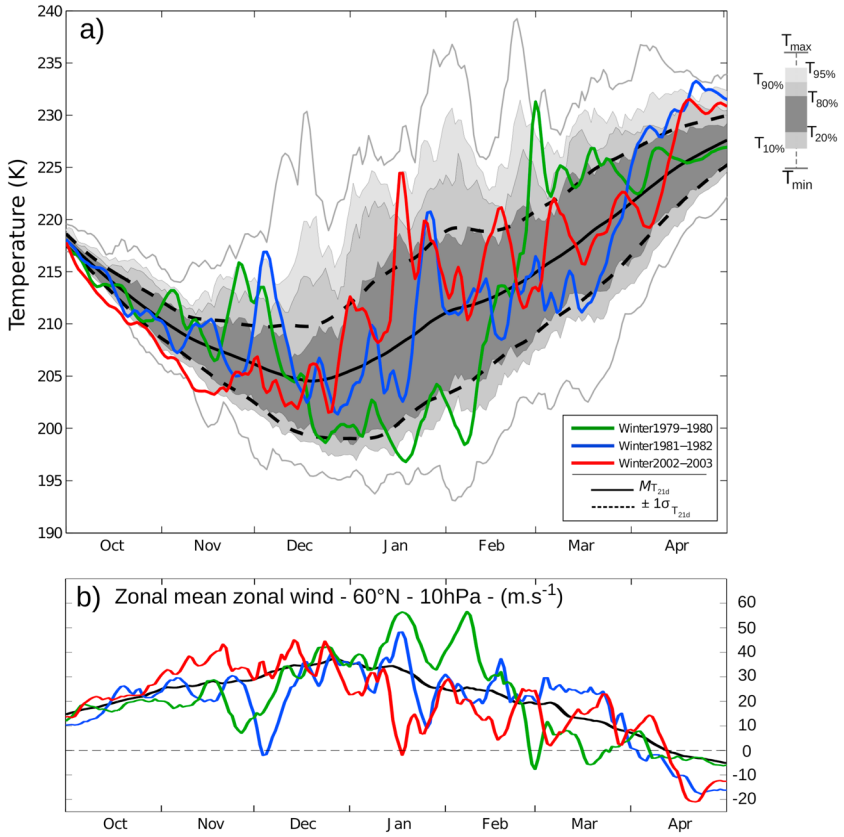

Figure 1. (a) Statistics of polar cap temperature averaged between 50 hPa and 10 hPa—$T(t_{d,y})$—evaluated from ERA reanalysis over 1959/1960 to 2012/2013 period. The grey-shaded area delimits (i) the $T_{20th}(t_d)$ to $T_{80th}(t_d)$ percentile values (dark grey), (ii) the $T_{10th}(t_d)$ to $T_{90th}(t_d)$ percentile values (medium grey), and (iii) the upper $T_{95th}(t_d)$ percentile value (light grey). The two light grey lines delimit the daily minimum $T_{min}(t_d)$ and maximum $T_{max}(t_d)$ of the temperature $T(t_{d,y})$. The thin black line denotes the 21 days running mean $\mathcal{M}_{T_{21d}}(t_d)$, and the two dashed black lines represent the 1 standard deviation departure to the mean. The green, blue, and red curves correspond to $T(t_{d,y})$ for the winters 1979–1980, 1981–1982, and 2002–2003, respectively. (b) Zonal mean zonal wind at 60°N and 10 hPa for the winters 1979–1980, 1981–1982, and 2002–2003 (green, blue, and red curves, respectively) and climatological mean (black line).

2.2. Stratospheric Warming Events

Stratospheric warmings are extracted by selecting only the days for which $\mathcal{I}_T(t_{d,y}) \geq +1$. Thereafter, a stratospheric warming event is defined by a set of consecutive days for which the criterion $\mathcal{I}_T(t_{d,y}) \geq +1$ remains satisfied, allowing to select 188 warming events over the 54 winters. Each stratospheric warming event is characterized by (i) a duration, (ii) an amplitude, (iii) a date of temperature maximum, d_{Tmax}, and (iv) the 5 day zonal mean zonal wind (60°N,10 hPa) minimum, $\overline{U}_{5d}$. The event duration $\mathcal{D}$ (in days) corresponds to the time during which the criterion $\mathcal{I}_T(t_{d,y}) \geq +1$ remains satisfied. The event amplitude $\mathcal{A}$ (in Kelvin) is calculated from the integral of the daily temperature deviation from the low-frequency mean, divided by the duration. For instance, considering a warming w_n, $\mathcal{A}(w_n)$ is evaluated following

$$\mathcal{A}(w_n) = \frac{1}{\mathcal{D}(w_n)} \int_{t_{d_i}}^{t_{d_f}} \left(T(t_{d,y_n}) - \mathcal{M}_{T_{21d}}(t_d) \right) \, \mathrm{d}t_d, \tag{2}$$

where t_{d_i} and t_{d_f},respectively, denote the first and the last days of the warming w_n. Over the duration of each event,d_{Tmax} corresponds to the day of the largest daily temperature and $\overline{U}_{5d}$ corresponds to a 5 day average of the zonal mean zonal wind at 60°N and 10 hPa around the date of zonal wind minimum.

The effectiveness of our approach is demonstrated by comparing the low-frequency standard deviation from the mean with the percentile values—$T_{pth}(t_d)$—evaluated from the daily temperature time series $T(t_{d,y})$ (Figure 1a, see legend for details). Note that the low-frequency standard deviation approximates the $T_{20th}(t_d)$ and $T_{80th}(t_d)$ percentile values (Figure 1a). Therefore, our stratospheric warming events comprise the upper

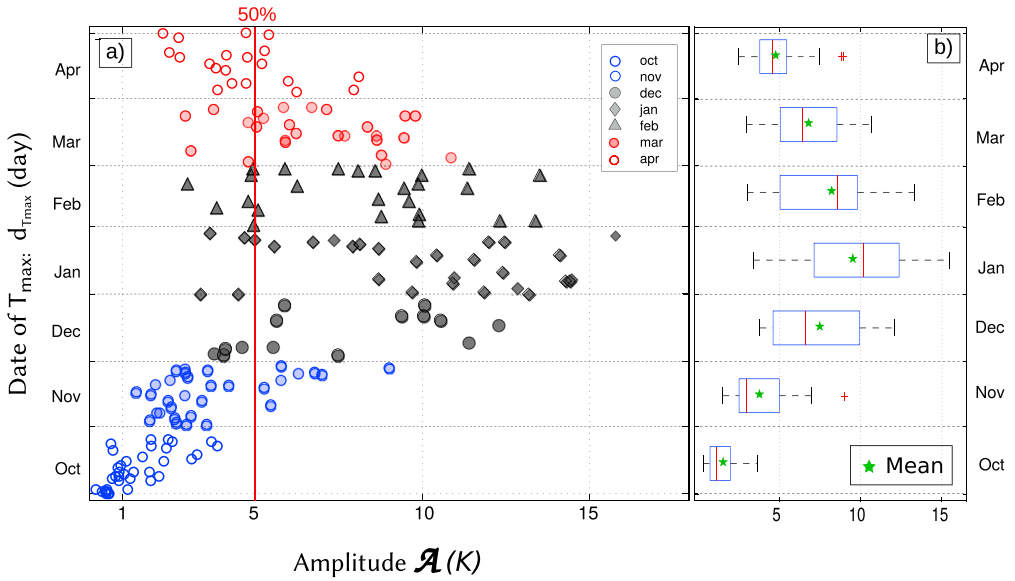

Figure 2. (a) The amplitude $\mathcal{A}$ of the warm events as a function of the date of temperature maximum d_{Tmax}. The red line corresponds to the median value. (b) Box-and-whisker plots of the warming amplitude for each month from October to April. The left and right sides of the boxes correspond to the first and third quartiles, respectively. The red band inside the box corresponds to the median, and the green star denotes the mean.

20th percentile of the temperatures. We thus selected large anomaly events, while not restricting our selection to the sole extreme events that are confined to the upper 5th or 10th percentile [*Stephenson et al.*, 2008]. A selection based on lower thresholds (0.5σ and 0σ) would include additional fluctuations. Such fluctuations would either increase the number of small amplitude and short events or extend the duration and lower the amplitude of the events (not shown). The latter effect is caused by an addition of days with small fluctuations before and after the events selected with 1σ threshold. The dependence reported in section 3.2 would therefore be blurred. The 1σ threshold appears to be the best compromise between maximizing the ensemble size and the rejection of small fluctuations.

Figure 1a also indicates that the temperature range between $T_{\mathrm{min}}(t_d)$ and $T_{\mathrm{max}}(t_d)$ is largest from December to February, minimal in October–November, and still relatively substantial in March–April, and evidences the well-known subseasonal variations in interannual variability. In addition, the larger temperature range between the high percentile $T_{80-90/95\mathrm{th}}(t_d)$ and $T_{\mathrm{max}}(t_d)$ in comparison with the temperature range between the low percentile $T_{10-20\mathrm{th}}(t_d)$ and $T_{\mathrm{min}}(t_d)$ indicates that over the 54 considered winters, strong temperature increases are more frequent than temperature decrease. This witnesses that the stratospheric temperature variability is dominated by strong warmings. To illustrate this point, the midstratospheric polar cap average temperature for three specific winters is added in Figure 1a. Independently of the winter considered, there is a large day-to-day variability, highlighted by sudden temperature rises, which occur more than twice a winter and exceed the $T_{80\mathrm{th}}(t_d)$ value. Finally, the zonal mean zonal wind at 60°N and 10 hPa for the three previous winters (Figure 1b) illustrates the strong anticorrelation between the wind and the temperature, confirming the using of $\overline{U}_{5d}$ as an indicator of the perturbation stage of the polar vortex.

3. General Characterization of Stratospheric Warmings

3.1. Warming Amplitude and Duration

To assess the characteristics of the warmings, the event amplitude is represented as a function of the date d_{Tmax} at which the warming maximum occurs (Figure 2a), together with the box-and-whisker plots to quantify the spread of the amplitude values for each month from October to April (Figure 2b). The amplitude of the warm events presents a seasonal dependence. All the October events and 75% of the November ones have amplitudes which never exceed 5*K*, whereas about 80% of the warmings occurring between December and February (DJF) have an amplitude larger than 5*K*, extending up to around 15*K*. During March, the mean and median of the event amplitudes are smaller than during January and February, and are similar to the ones in December, but the probability to have larger amplitude events in December is higher than in March.

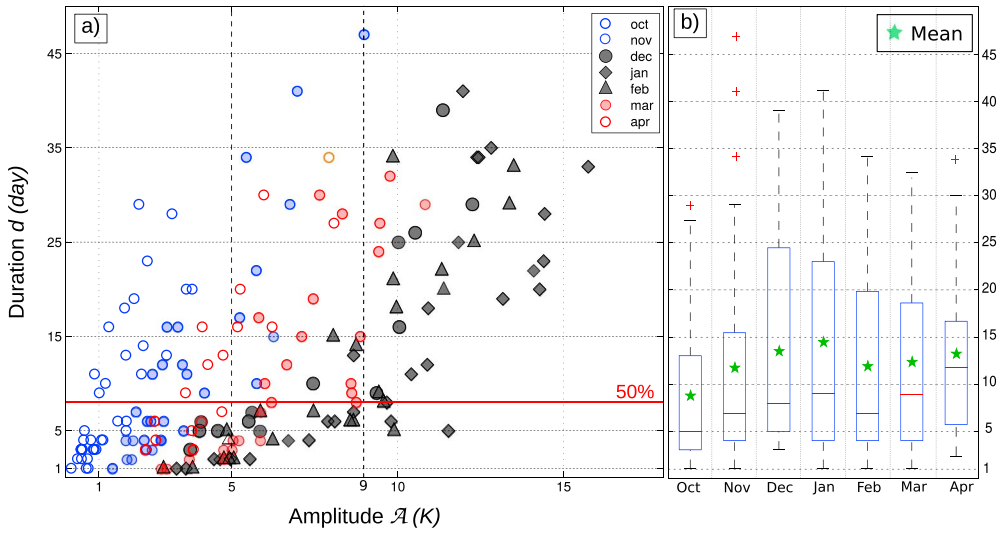

Figure 3. (a) The amplitude $\mathcal{A}$ of the warm events as a function of the duration $\mathcal{D}$. The color code is the same as in Figure 2a. (b) Box-and-whisker plots as in Figure 2b but for the duration.

In April, around 75% of the warmings have an amplitude less than 5*K*, like in November. The box size is larger for DJF than for the other months, indicating a larger spread of the amplitude values for the DFJ warmings than the October–November or March–April warmings.

When the amplitude is reported as a function of the duration, a large correlation is observed between both (Figure 3a). Overall, the duration of the warmings increases with the amplitude, but this correlation is dependent on season. For instance, warmings with amplitudes $5K<\mathcal{A}<9K$ tend to be longer in November, March, and April compared to those occurring in DJF. For November this can be explained by a longer radiative damping time than in DJF [*Newman and Rosenfield*, 1997], but this does not apply for March–April. Compared to midwinter period, $5K<\mathcal{A}<9K$ amplitude warmings may be large enough to disturb durably the late-winter vortex. Indeed, due to the strong midwinter vortex, the stratospheric circulation may return faster to its climatological state than during late winter.

Figure 4 shows the probability density function (PDF) of the event amplitude (i.e., the *x* axis in Figure 2a) and duration (i.e., the *y* axis in Figure 3a). The PDF of the amplitudes reveals a bimodal distribution with two relative maxima. The first relative maximum is a broad peak at low amplitudes ($\mathcal{A}<5K$), approaching the amplitude median value, and the second one is at around 9*K* and delimits the upper 20% of the larger-amplitude warm events. When the early wintertime (October to mid-November), the midwintertime (mid-November to mid-March), and the late wintertime (mid-March to April) are considered separately, Figure 4a reveals a subseasonal dependence of the frequency in amplitude values. The first warming set ($\mathcal{A}\leq 5K$) mainly consists of (i) early-winter warmings and (ii) around the half of late-winter warmings. Conversely, the second warming set ($\mathcal{A}>5K$) mainly consists of midwinter warmings and the other half of late-winter warmings. Note that the secondary peak is almost exclusively explained by midwinter events. The PDF of the event duration (Figure 4b) is rather sharply decreasing for small-duration values, given that 50% of the selected events last less than 10 days (Figure 3a, and see also the positive skewness seen in Figure 3b). Although less pronounced than for the amplitude values, the PDF of event duration also hints at bimodality. This possibility is more apparent for the midwinter PDF (break point around 20 day duration and a second maximum at around 30 day duration).

3.2. Warm Events and the Stratospheric Polar Vortex

In this section, the temporal distribution of warm events is analyzed together with the stage of the polar vortex during the events. Figure 5 reports the warm events as a function of the date d_{Tmax} with their amplitude and duration, stratified according to their amplitude ($\mathcal{A}\leq 5K$, $5K<\mathcal{A}\leq 9K$, and $\mathcal{A}>9K$, see legend for details). The daily values of the zonal mean zonal wind at 60°N and 10 hPa are also superimposed in Figure 5 for the 54 winters.

3.2.1. Case Distribution Over the Winters

The total frequency of the event occurrence by winter (3.8) is quasi uniformly distributed over the 54 winters (not shown). Main differences between winters come from the numbers of small amplitude ($\mathcal{A}\leq 5K$) warmings

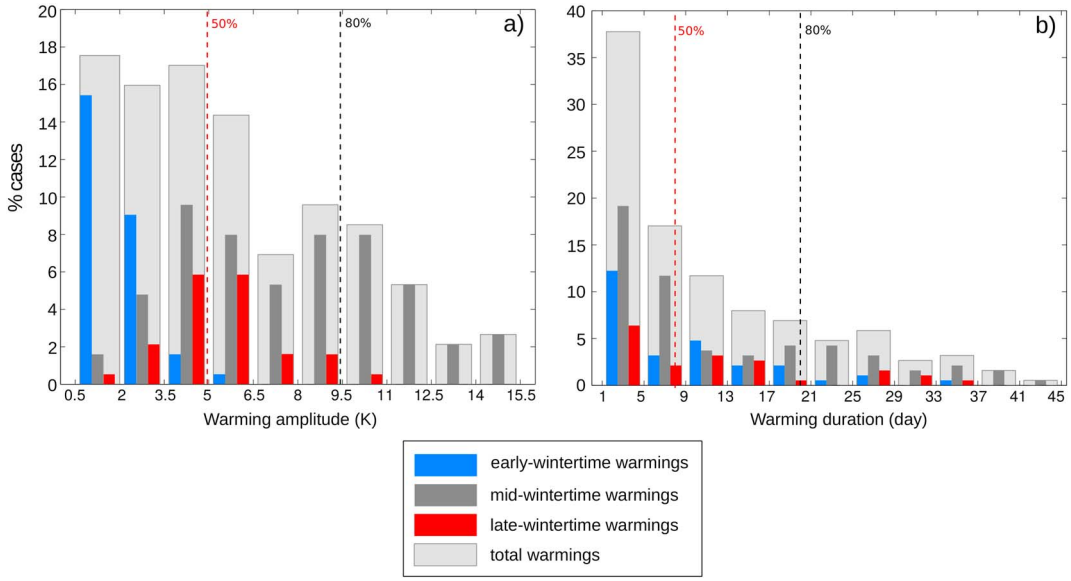

Figure 4. Probability density function of (PDF) (a) warming amplitudes $\mathcal{A}$ and (b) durations $\mathcal{D}$. Light grey histograms are for total events, and histograms in blue, dark grey, and red correspond to warming distribution of early (October to mid-November), mid (mid-November to mid-March), and late wintertime (mid-March to April), respectively. Red dashed lines represent the median, and the black dashed lines the 80th percentile value.

(see, for instance, winters 1971–1972 and those from 1990 to 1994). As already noticed in Figure 2, these small amplitude events ($\mathcal{A} \leq 5K$) mainly occur during October, November, and April, and they tend to happen twice or more in a short time period. For larger amplitude events ($\mathcal{A} > 5K$) there are two distinct distributions of events according to their duration. Short-time events are essentially occurring closely to other events (e.g., December/January 1975/1976 to January/February 1991), whereas long-time ones are rather "isolated"

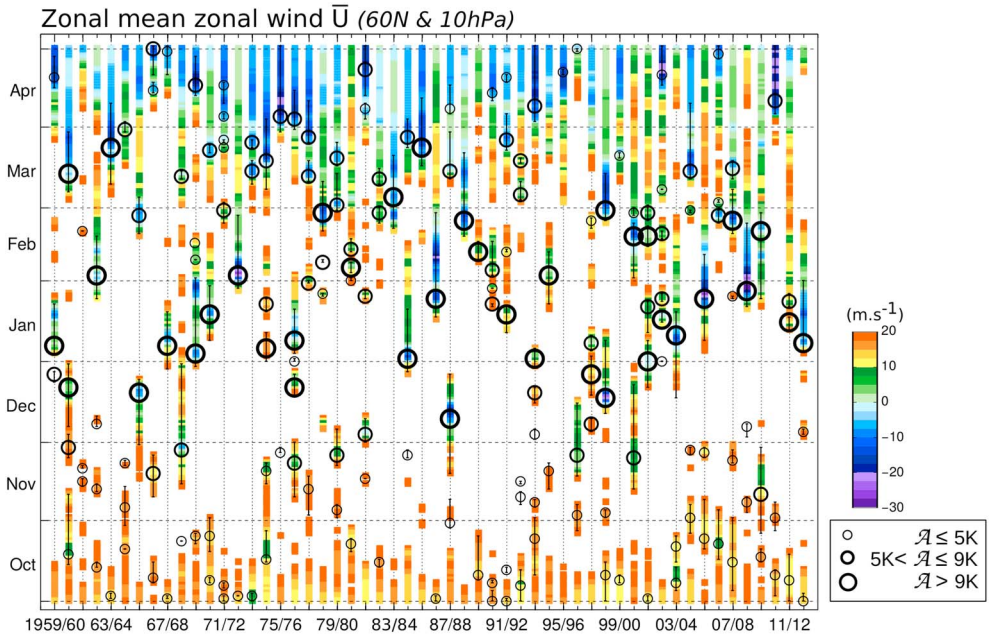

Figure 5. Warming events are represented as a function of the date d_{Tmax} and the year by a circle. The size of the circles depends on the amplitude ($\mathcal{A} \leq 5K$, $5K < \mathcal{A} \leq 9K$, and $\mathcal{A} > 9K$) and vertical black lines indicate the duration. The zonal mean zonal wind at 60°N and 10 hPa $\overline{U}$ is also superimposed for the 54 winters from October 1959 to April 2013 (daily values). Negative zonal wind values are in blue/purple for $\overline{U} \leq 0$ m s^{-1}. Weak vortex are in green and orange for wind value $0 < \overline{U} \leq 10$ m s^{-1} and $10 < \overline{U} \leq 20$ m s^{-1}, respectively. Strong vortex with $\overline{U} > 20$ m s^{-1} are in white.

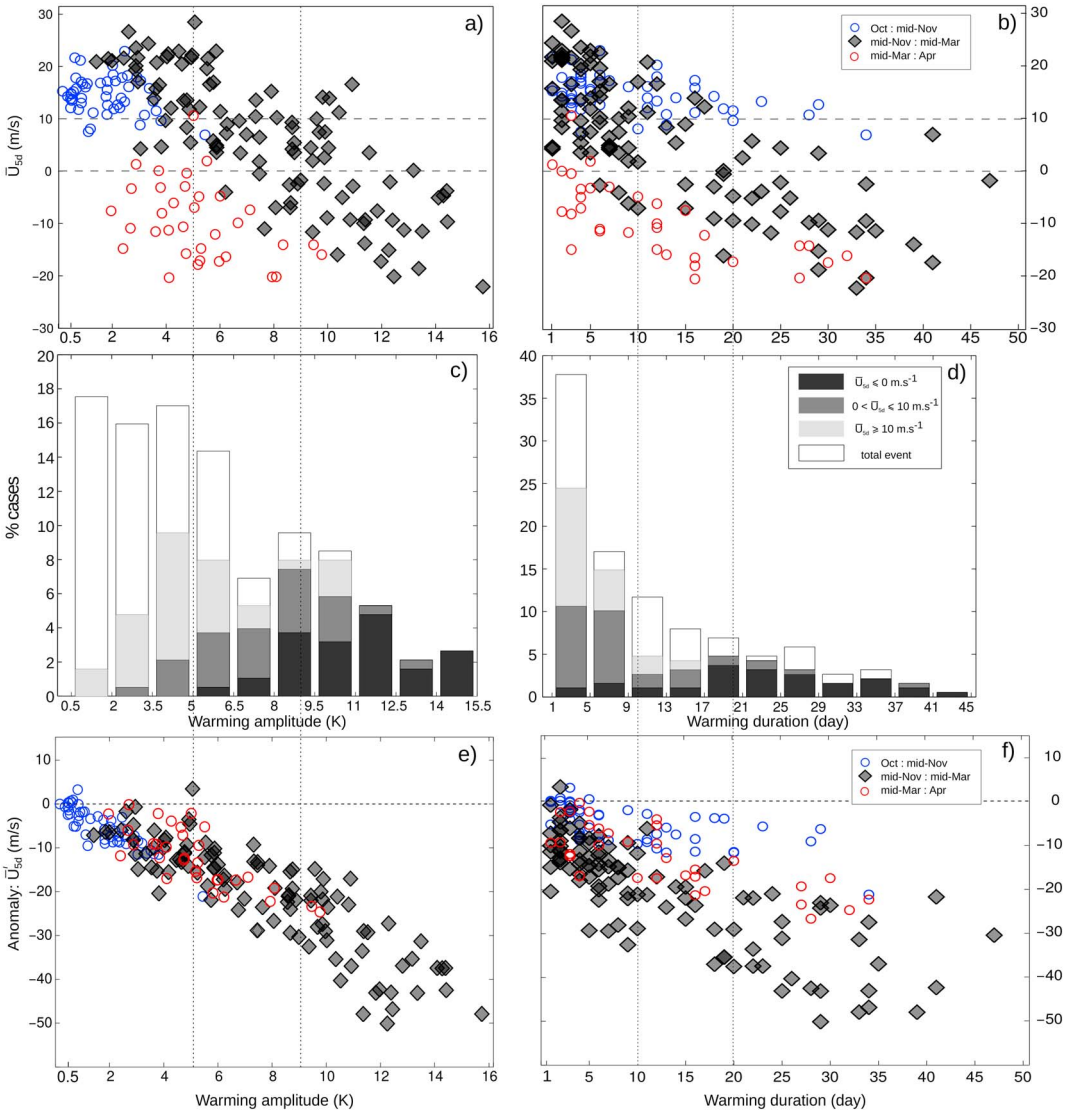

Figure 6. (a) Amplitude and (b) duration for each warm event as a function of the 5 day zonal wind minimum $\overline{U}_{5d}$. Blue markers for early-winter (October to mid-November) events, black markers for midwinter (mid-November to mid-March) events, and red markers for late-winter (mid-March to April) events. The PDF of (c) the amplitude and (d) the duration for all the events (white, as in Figure 4), and the midwinter events stratified according to the $\overline{U}_{5d}$ wind values: with $\overline{U}_{5d} \leq 0$ m s^{-1} (dark grey), $0 < \overline{U}_{5d} \leq 10$ m s^{-1} (medium grey), and $\overline{U}_{5d} > 10$ m s^{-1} (light grey). (e) Warming amplitude and (f) duration as a function of the anomaly of $\overline{U}_{5d}$.

(e.g., February 1963 to January 1985). Note that during the second part of November, warm events with $5K < \mathcal{A} \leq 9K$ last more than 10 days and are isolated like in DJF (see, for instance, in November 1968 or 1996). Because the time between two closely occurring consecutive warmings is generally less than 20 days (not shown), it is natural to interpret such a group of events as a response to pulses of planetary wave activity [*Zhou et al.*, 2002]. Such successive warm events are thus not independent from each other and belong to the same perturbation stage of the polar vortex, and we label them "clustered events." This interpretation is supported by the zonal wind value associated to each clustered events (e.g., December/January 1976–1977 or January/February 1991).

3.2.2. Stratospheric Polar Vortex

Figure 5 suggests that a distinct seasonal dependence between the amplitude of the events and the strength of the polar vortex tend to be related to a weak vortex during November (around 10 m s^{-1}) but to a total wind reversal at the end of the winter in March and April due to the vortex decay. In the same way, events with $\mathcal{A} \leq 5K$ are associated with zonal wind values of 15–20 m s^{-1} during October and the first part of November,

but with negative wind values during the second part of March and April. These small events are indicative of some fluctuations of the vortex intensity during the polar vortex strengthening (early winter) or decay (late winter) but do not lead to dramatic vortex perturbations. On the opposite, during midwinter the warmings with $\mathcal{A} \geq 5K$ are generally accompanied with dramatic vortex perturbations. The majority of the warmings having $\mathcal{A} \geq 9K$ are associated with a total vortex breakdown, whereas events with $5K < \mathcal{A} \leq 9K$ (medium circles) are mainly associated to a weak polar vortex, with zonal mean zonal wind around 10 m s^{-1}. However, the amplitude value of $\mathcal{A}=9K$ is not a well-defined threshold to separate the events into two different vortex states. Indeed, large warming amplitudes can also be associated with a weak vortex (i.e., in February 1981 or during January–February 1989–1994). Conversely, medium-amplitude events can be associated with a total wind reversal (i.e., February 1966 to November 1968 to February 2007).

To clarify the linkage between the event amplitude/duration and zonal wind by season, in Figure 6 the events are grouped according to the three winter periods: early, mid, and late winter. Figures 6a and 6b show a strong correlation between the 5 day zonal wind minimum $\overline{U}_{5d}$ and both amplitude and duration for the midwinter events. Both figures confirm that early- and late-wintertime events do not show the same relationship between amplitude or duration and the wind $\overline{U}_{5d}$ than for the midwintertime events. Thus, only midwintertime events are considered to build the PDF of the amplitude and duration, stratified according to the value of $\overline{U}_{5d}$ (Figures 6c and 6d). Figure 6c shows that the median value $\mathcal{A}=5K$ tends to separate the midwinter events according to the wind value $\overline{U}_{5d}=10$ m s^{-1}. Considering only the events with $\overline{U}_{5d} \leq 10$ m s^{-1}, a bell-shaped "continuum" of stratospheric warming emerges, instead of two distinct stratospheric winter states where minor and major SSWs are separated. This result corroborates the idea of warming continuum outlined in *Coughlin and Gray* [2009], expanding their results to a larger sample of events. Concerning duration, Figure 6d shows that the warm events associated to a total vortex breakdown tend to have longer duration than events associated to a weak vortex, 70% of the latter persisting less than 10 days. The warming duration could therefore be a condition to discriminate most of the minor SSWs from the major ones. This result is possibly consistent with the correlation between the depth and the duration of the warmings found by *Hitchcock et al.* [2013]. Interestingly, when considering wind anomalies instead of absolute wind values, a correlation with the warming amplitude is observed, independently of the winter season (Figure 6e). On the contrary, the correlation between the warming duration and the wind anomalies remains seasonal dependent (Figure 6f).

4. Focus on the Strong Events

4.1. Selection of Events

The analysis of the previous section has demonstrated that the median amplitude value $\mathcal{A} = 5K$ divides the events into two groups that present both distinct seasonal and dynamical properties. We therefore chose $\mathcal{A} > 5K$ as our threshold for large-amplitude events in the following. In addition, closely occurring events with an interwarming time lower than 20 days have been merged together. After this selection and merging, the number of stratospheric warming events is reduced to about 40%. We call this new set of events the strong (stratospheric) warming events (SWE).

4.2. Meridional Heat Flux

The meridional heat flux $\overline{v'T'}$ is a fundamental quantity for understanding the Northern Hemisphere stratosphere behavior [*Newman and Nash*, 2000]. The heat flux $\overline{v'T'}$ at 100 hPa averaged between 55°N and 80°N [see *Andrews et al.*, 1987] is presented in Figure 7. Superimposed to the heat flux, the SWEs are depicted in terms of their amplitude, duration, and sign of $\overline{U}_{5d}$. The meridional heat flux is larger from December to March, mainly positive, indicating an upward wave propagation from the troposphere, and presents interannual variability correlated with the occurrence of SWEs, coherently with *Polvani and Waugh* [2004]. Visual inspection of Figure 7 shows that, independently of the event amplitude, the heat flux tends to be large before the date of maximum temperature of SWEs and drastically decreases thereafter. In a number of cases, the heat flux actually becomes negative after the day d_{Tmax}. The meridional heat flux, being directly proportional to the vertical component of the Eliassen Palm flux [*Andrews et al.*, 1987], informs of the planetary wave propagation through the atmosphere [*Pawson and Kubitz*, 1996; *Newman et al.*, 2001]. In this way, a positive eddy heat flux indicates that waves propagate vertically from the troposphere to the stratosphere, and conversely, a negative eddy heat flux indicates a downward propagation of planetary waves to the troposphere [*Perlwitz and Harnik*, 2003]. As outlined by *Kodera et al.* [2013, 2016], a negative meridional heat flux after a major SSWs can therefore indicate reflection of planetary waves by the perturbed polar vortex. Such a wave reflection leads to an

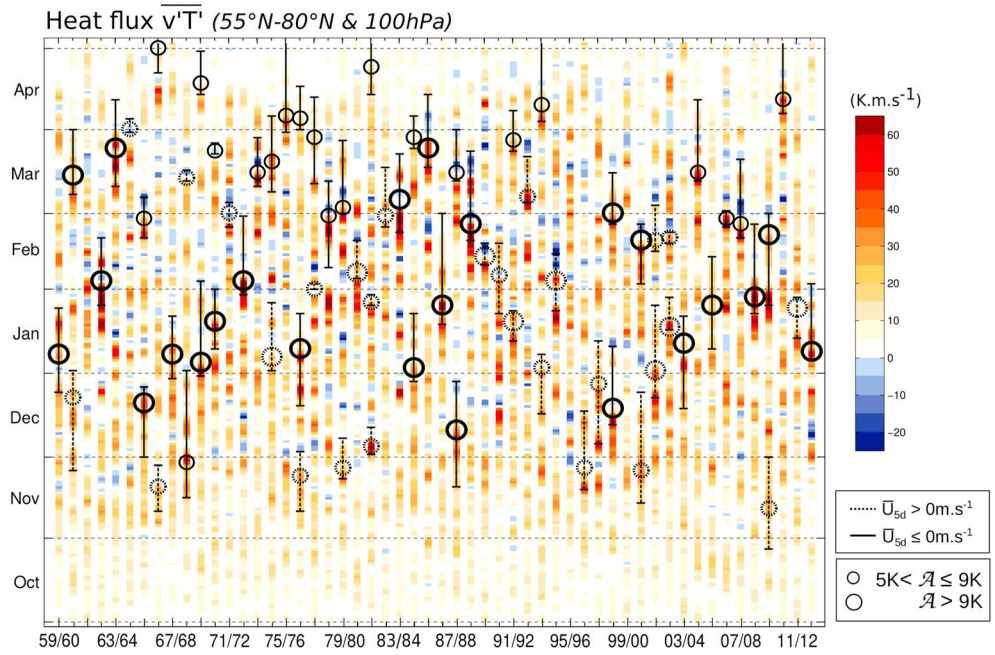

Figure 7. Meridional heat flux at 100 hPa averaged between 55°N and 80°N over the 54 winters from October 1959 to April 2013 (daily values). The warm (cold) colors indicate positive (negative) heat flux. The SWEs are superimposed. The size of the circles depends on the amplitude with medium ($5K<\mathcal{A}\leq 9K$) and large ($\mathcal{A}>9K$). Also, solid (dashed) circles correspond to events with a negative (positive) $\overline{U}_{5d}$. Black lines indicate the warmings duration.

amplification of the tropospheric planetary wave structure inducing strong westerlies over the North Atlantic and blocking over the North Pacific sector and thus impact tropospheric weather [*Kodera et al.*, 2016]. Interestingly, Figure 7 demonstrates that a negative meridional heat flux can also appear thereafter; SWEs without a wind reversal (see, for instance, March 1972 or February 1990). This observation suggests that some minor SSWs could also lead to tropospheric impacts.

4.3. Composite of Meridional Heat Flux Anomalies

Composites of heat flux anomalies have been evaluated for the midwinter SWEs with $5K<\mathcal{A}\leq 9K$ and $\mathcal{A}>9K$ separately, centered at the date d_{Tmax} corresponding to the lag = 0 day. Composites show a significant difference about 10 days before lag = 0 where a larger forcing is observed for events with $\mathcal{A} > 9K$ compared with events with $5K<\mathcal{A}\leq 9K$ (Figure 8, red and orange curves). However, surprisingly, there is no significant difference between the two composites from lag = −5 day to lag = 25. In the case of a vortex breakdown, waves can no longer propagate upward [*Charney and Drazin*, 1961], explaining drop in the composite of heat flux

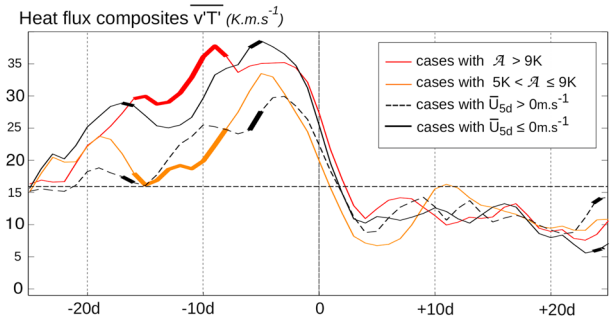

Figure 8. Midwinter meridional composites of heat flux anomalies (100 hPa; 55°N–80°N) over a 51 day windows, centered on the date d_{Tmax}. Orange and red lines correspond to composites for warmings with $5K<\mathcal{A}\leq 9K$ and $\mathcal{A} > 9K$, respectively. Black and grey lines stand for composite for warmings with $\overline{U}_{5d} \leq 0$ m s^{-1} and $\overline{U}_{5d} > 0$ m s^{-1}, respectively. Bold lines indicate the days where the composites of heat flux anomalies statistically differ from the climatology with the 95% significant level according to a Student's *t* test. The light (dark) grey shaded area indicates days where the composites stratified by the amplitude (zonal wind) differ with the 95% significant level according to a Student's *t* test.

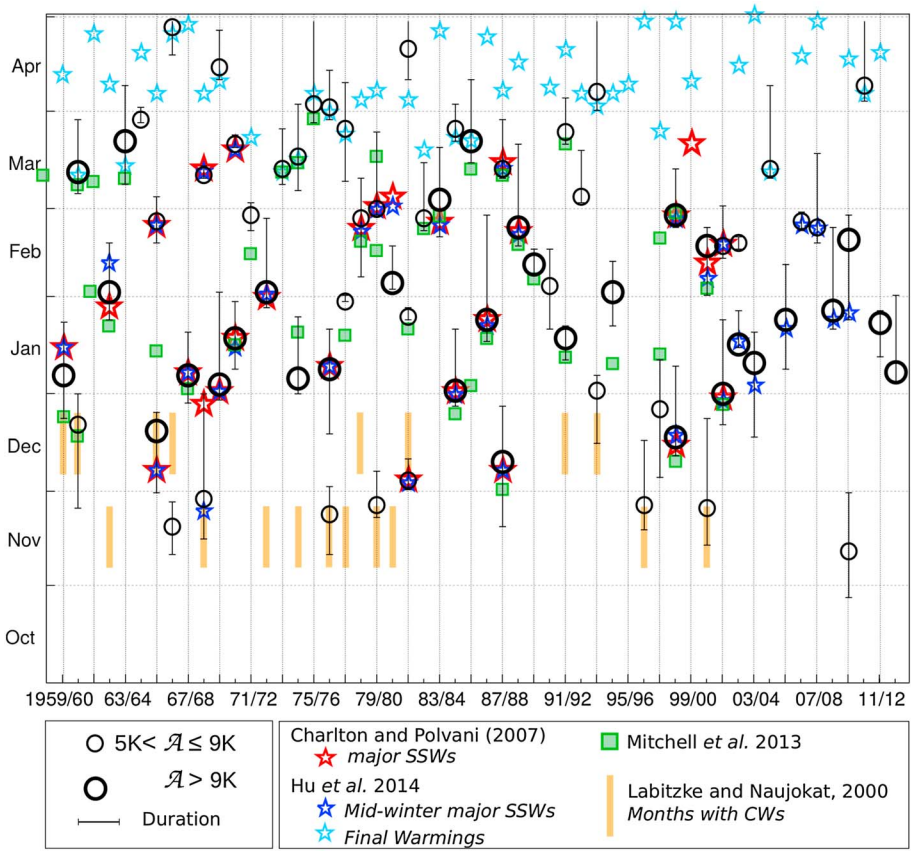

Figure 9. SWEs distribution contrasted with SSWs climatologies. SWEs are represented by black circles where the size depends on the amplitude value, and vertical black lines indicate the duration (see Figure 7). Cases listed in (i) CP07 are represented by red stars, (ii) Mi12 by green squares, and (iii) Hu14 by blue stars for midwinter warmings (dark blue) and final warmings (light blue). Months with Canadian warmings described in LN00 are marked by vertical orange lines.

anomaly for events with $\mathcal{A}>9K$, given that they are mostly made of major SSWs. But the composite for events with $5K<\mathcal{A}\leq 9K$ is not statistically different from the one with $\mathcal{A}>9K$, whereas this population of events is mainly associated with minor SSWs. To demonstrate the insensitivity to the sign of the zonal wind in the heat flux evolution for the SWEs, two additional composites are shown, for which the SWEs are stratified according to the sign of $\overline{U}_{5d}$ (black and grey lines in Figure 8). Although the forcing and the degree of vortex perturbation (implied by the sign of $\overline{U}_{5d}$) differ between the events, their feedback on the planetary waves is comparable. Indeed, after the lag = 0 and on the entire period (up to lag = +25) the heat flux drops below the climatology for all cases. This result suggests that a total wind reversal is not a requirement for the wave activity to drop significantly. Therefore, the dynamics of a perturbed vortex cannot be distinguished by the sign of the zonal wind, corroborating the idea of a "continuum" of SSWs.

4.4. Comparison With Published "SSW Climatologies"

This part intends to compare the SWEs with published lists of SSWs. Such lists have been presented by *Charlton and Polvani* [2007] (CP07), *Mitchell et al.* [2012] (Mi12), *Hu et al.* [2014] (Hu14), and *Labitzke and Naujokat* [2000] (LN00). CP07 identify SSWs following the zonal mean zonal wind reversal at 60°N and 10 hPa, whereas Mi12 use a method based on a vortex moment analysis. Both studies use the ERA-40 reanalysis from winter 1957–1958 to 2000–2001. Hu14 identify major SSWs by looking for positive meridional temperature gradient northward to 60°N at 10 hPa and a zonal mean zonal wind reversal at 65°N, with NCEP-NCAR reanalysis from winter 1957–1958 to 2011–2012 [*Kalnay et al.*, 1996]. As we use the extended wintertime season from October to April, the occurrence of our early- and late-winter SWEs can be compared to the Canadian warming (CW) and Final warming (SFW) listed in LN00 and Hu14, respectively. Note that for the CW list, only the months when the warmings occur are available. The comparison between the early-winter SWEs and CWs is justified because many of them are considered as CW [*Labitzke*, 1977].

The frequency of occurrence of the SWEs is around ∼1.8 events a year, against ∼0.6/0.65 in CP07/Hu14, and close to one event a year in Mi12. Clearly, these differences are related to the inclusion of the events usually termed as minor SSW (here and in Mi12) by a textbook definition [*Andrews et al.*, 1987]. Also, we consider early- and late-winter SWEs without distinction neither between midwinter SSWs and SFWs nor between early/midwinter and CWs, whereas CP07, Hu14, and Mi12 make this distinction between their events. To contrast the SWEs presented here with other climatologies of SSWs, our selected events are represented in Figure 9 as a function of the day and the year, together with events listed in CP07, Hu14, Mi12, and LN00.

Canadian warmings. Among the 18 CWs listed by LN00, about 65% (11 CWs) are indeed selected. Note that, because LN00 only report the month where the CWs happened and not the date, the SWE occurring in November 1966 is considered as the CW occurring in December 1966. The 35% missing are likely due to the fact that CWs are mainly associated with small anomalous temperatures in the lower levels of the stratosphere [*Manney et al.*, 2001]. For instance, CWs in November 1962 and December 1978 are associated with a warm anomaly that occurs below 50 hPa (not shown), while our selection is based on a (pressure-weighted) temperature average between 50 and 10 hPa.

Midwinter events. Most of the major SSWs identified by CP07 (red stars) and Hu14 (dark blue stars) coincide with the SWEs, except for the case of 20 March 2000 (only selected by CP07). This particular SSW has a short time period of zonal wind reversal and a positive temperature anomaly confined above 20 hPa (not shown), precluding its selection by our method. It is important to note that the trend toward a diminution of SSW activity during the 1990s [*Pawson and Naukojat*, 1999, CP07] is not clearly observed in Figure 9. In agreement with Mi12, SWEs are indeed observed during this decade, even though most of them are considered as minor warmings. Moreover, this observation remains consistent with *Butler et al.* [2015], reporting warm events during the 1990s for the methods used in *Gerber et al.* [2010] and *Limpasuvan et al.* [2004].

Final warmings. It is important to recall that SFWs happen at the end of the winter during the transition between winter (westerly winds) and summer (easterly winds) circulation. However, only about 30% of the SFWs listed in Hu14 are identified in our analysis. According to Figure 5, the selected late-winter SWEs are accompanied by a drastic wind deceleration whereas SFWs identified by Hu14 are not systematically associated with such a wind deceleration but rather to a smooth transition to easterly winds. Also, Figure 7 shows an enhanced heat flux as precursor for most of the late-winter SWEs identified here, whereas the heat flux is weak for most of the unselected SFWs listed in Hu14. This indicates that our method seems to discriminate SFWs due to a dynamical forcing, which can be considered as *"sudden"* SFWs and prevent the vortex recovery before the spring, from those — unselected — due to radiative processes [*Sun and Robinson*, 2009].

5. Summary and Conclusion

This work investigated the occurrence of stratospheric warming events, from the beginning of October to the end of April, in an extended reanalysis data set based on the merging of ERA-40 and ERA-I. Two selection criteria have been used to select the stratospheric warming events. The first one provides a general description of temperature variability in the stratosphere, including nonextreme events (section 3). The second one, a more restrictive criterion, is based on the statistical properties of the warming set and on dynamical considerations associated with them, and aims at investigating whether there is a clear separation between major SSWs and minor SSWs (section 4).

The first selection criterion was used to characterize stratospheric warming events in terms of amplitude, duration, and occurrence. A bimodality in the distribution is found for the event amplitude, with each subdistribution amounting to about half of the total events. The amplitude distribution with $\mathcal{A} \leq 5K$ mostly consists of early- and late-winter events, whereas the distribution with $\mathcal{A} > 5K$ mostly consists of midwinter events and has a sharper amplitude maximum at $9K$. Diagnostics of the zonal mean zonal wind reveal that both amplitude and duration of the warmings correlate with the zonal wind, for events occurring from mid-November to mid-March. During this winter period, the majority of events associated with a weak zonal wind (minor SSWs) and the totality of events with negative zonal winds (major SSWs) have also an amplitude $\mathcal{A} > 5K$. Within our statistics, the threshold of $\mathcal{A} > 5K$ therefore separates warm events with distinct dynamical properties. We attribute the seasonal dependence of the warming amplitude to the climatological vortex dynamics that evolves during the wintertime due to the polar night. This seasonal dependence is not as clear in the case of the warming duration. However, our analysis reveals that major SSWs tend to be longer-lived events than minor SSWs.

The second selection criterion allows for selecting the "strong (stratospheric) warming events (SWEs)", including both major and minor SSWs, and also Canadian warmings (CWs, LN00) and a subsection of Final warmings (SFWs, Hu14). Our method therefore succeeds in a broad characterization of stratospheric variability that is not only restricted to the extreme variability. Moreover, our method allows the selection of SFWs that are likely dynamically driven rather than resulting from radiative processes [*Sun and Robinson*, 2009]. Among the selected SWEs, the midwinter ones — associated with a $\overline{U}_{5d} \leq 10\ \mathrm{m\ s^{-1}}$ — can be described as a "warming continuum," without distinction between the different SSW types. This result confirms the conclusion of *Coughlin and Gray* [2009] who introduced the existence of a warming continuum and extends it to a wider range of events.

Diagnostics of heat flux anomalies demonstrate that for both major and minor SSWs the heat flux drops below the climatology after the warmings peak. This result suggests that a total wind reversal is not a strict prerequisite for the wave activity to drop significantly. This drop can not be explained by a simple application of the theory of *Charney and Drazin* [1961], as observed by *Hitchcock et al.* [2013]. The warming continuum observed here explains both (i) the difficulties in developing a standard definition for SSWs [*Butler et al.*, 2015] and (ii) the discrepancies between the SSWs selected by different protocols [*Palmeiro et al.*, 2015]. Because we demonstrate that minor SSWs are not fundamentally different from the major ones, classifications of SSWs based on the wind reversal become questionable. Thereafter, minor SSWs may be as important as major SSWs in terms of dynamical coupling perspectives between stratosphere and troposphere, for instance, via stratospheric waves reflection [*Kodera et al.*, 2016].

Finally, as our method is an easily derived diagnostic, based on only one variable (the temperature), the statistics presented here can be very useful in the context of evaluating atmospheric models. Previous model evaluations only focused on major SSWs and revealed large discrepancies in the occurrence of major stratospheric warmings [*SPARC*, 2010; *Charlton-Perez et al.*, 2013]. This new diagnostic and a more extensive analysis of the stratospheric warmings may help to reduce and/or understand model biases in variability and their consequences. In a more general view, it is expected that the present contribution should help both to evaluate the simulation of the dynamical interaction between SSWs and the background flow in models and to study the effect of changes in both extreme and nonextreme variabilities and SSWs on the stratospheric response to global warming.

Acknowledgments
The ERA-40 and ERA-Interim atmospheric reanalysis data have been obtained from ECMWF (http://www.ecmwf.int/en/research/climate-reanalysis). This work was supported by the French National Research Agency (ANR) through the StraDyVariUS project, ANR-13-BS06-0011 and by the Chaire de Développement Durable of the Ecole Polytechnique-EDF. The authors would like to acknowledge the helpful comments and feedbacks on the manuscript by K. Kodera, T. Reichler, and the anonymous reviewer.

References

Andrews, D. G., J. R. Holton, and C. B. Leovy (1987), *Middle Atmosphere Dynamics*, Harcourt Brace Jovanovich, Academic Press, New York.
Butler, A., D. Seidel, S. Hardiman, N. Butchart, T. Birner, and A. Match (2015), Defining sudden stratospheric warmings, *Bull. Am. Meteorol. Soc.*, *96*, 1913–1928, doi:10.1175/BAMS-D-13-00173.1.
Charlton, A. J., and L. M. Polvani (2007), A new look at stratospheric sudden warmings. Part I: Climatology and modeling benchmarks, *J. Clim.*, *20*, 449–469.
Charlton-Perez, A. J., et al. (2013), On the lack of stratospheric dynamical variability in low-top versions of the CMIP5 models, *J. Geophys. Res. Atmos.*, *118*, 2494–2505, doi:10.1002/jgrd.50125.
Charney, J. G., and P. G. Drazin (1961), Propagation of planetaryscale disturbances from the lower into the upper atmosphere, *J. Geophys. Res.*, *66*, 83–109.
Cohen, J., and J. Jones (2011), Tropospheric precursors and stratospheric warmings, *J. Clim.*, *24*, 6562–6572, doi:10.1175/2011JCLI4160.1.
Coughlin, K., and L. J. Gray (2009), A continuum of sudden stratospheric warmings, *J. Atmos. Sci.*, *66*, 531–540, doi:10.1175/2008JAS2792.1.
Dee, D. P., et al. (2011), The ERA-Interim reanalysis: Configuration and performance of the data assimilation system, *Q. J. R. Meteorol. Soc.*, *137*, 553–597, doi:10.1002/qj.828.
SPARC (2010), SPARC CCMVal Report on the Evaluation of Chemistry-Climate Models, *SPARC Rep. 5, WCRP-30/2010, WMO/TD-40*, edited by V. Eyring, T. Shepherd and D. Waugh. [Available at www.sparc-climate.org/publications/sparc-reports/.]
Gerber, E. P., C. Orbe, and L. M. Polvani (2009), Stratospheric influence on the tropospheric circulation revealed by idealized ensemble forecasts, *Geophys. Res. Lett.*, *36*, L24801, doi:10.1029/2009GL040913.
Gerber, E. P., et al. (2010), Stratosphere-troposphere coupling and annular mode variability in chemistry-climate models, *J. Geophys. Res.*, *115*, D00M06, doi:10.1029/2009JD013770.
Hitchcock, P., and T. G. Shepherd (2013), Zonal-mean dynamics of extended recoveries from stratospheric sudden warmings, *J. Atmos. Sci.*, *70*, 688–707, doi:10.1175/JAS-D-12-0111.1.
Hitchcock, P., T. G. Shepherd, and G. L. Manney (2013), Statistical characterization of Arctic polar-night jet oscillation events, *J. Clim.*, *26*, 2096–2116, doi:10.1175/JCLI-D-12-00202.1.
Hu, J., R. Ren, and H. Xu (2014), Occurrence of winter stratospheric sudden warming events and the seasonal timing of spring stratospheric final warming, *J. Atmos. Sci.*, *27*, 2319–2334, doi:10.1175/JAS-D-13-0349.1.
Kalnay, E., et al. (1996), The NCEP/NCAR 40-year reanalysis project, *Bull. Am. Meteorol. Soc.*, *77*, 437–471, doi:10.1175/1520-0477.
Karpechko, A. Y., and E. Manzini (2012), Stratospheric influence on tropospheric climate change in the Northern Hemisphere, *J. Geophys. Res.*, *117*, D05133, doi:10.1029/2011JD017036.
Kodera, K., Y. Kuroda, and S. Pawson (2000), Stratospheric sudden warmings and slowly propagating zonal-mean zonal wind anomalies, *J. Geophys. Res.*, *105*(D10), 12,351–12,359.
Kodera, K., H. Mukougawa, and A. Fujii (2013), Influence of the vertical and zonal propagation of stratospheric planetary waves on tropospheric blockings, *J. Geophys. Res. Atmos.*, *118*, 8333–8345, doi:10.1002/jgrd.50650.

Kodera, K., H. Mukougawa, P. Maury, M. Ueda, and C. Claud (2016), Absorbing and reflecting sudden stratospheric warming events and their relationship with tropospheric circulation., *J. Geophys. Res. Atmos.*, *121*(80–94), doi:10.1002/2015JD023359.
Kuroda, Y., and K. Kodera (2004), Role of the polar-night jet oscillation on the formation of the Arctic oscillation in the Northern Hemisphere in winter, *J. Geophys. Res.*, *109*, D11112, doi:10.1029/2003JD004123.
Labitzke, K. (1977), Interannual variability of the winter stratosphere in the Northern Hemisphere, *Mon. Weather Rev.*, *105*, 762–770.
Labitzke, K., and B. Naujokat (2000), The lower arctic stratosphere in winter since 1952, *SPARC Newslett.*, *15*, 11–14.
Limpasuvan, V., D. W. J. Thompson, and D. L. Hartmann (2004), The life-cycle of the Northern Hemisphere sudden stratospheric warmings, *J. Clim.*, *17*, 2584–2596.
Manney, G. L., J. L. Sabutis, and R. Swinbank (2001), A unique stratospheric warming event in November 2000, *Geophys. Res. Lett.*, *28*, 2629–2632.
Matsuno, T. (1971), A dynamical model of the stratospheric sudden warming, *J. Atmos. Sci.*, *28*, 1479–1494.
McInturff, R. (1978), *Stratospheric Warmings: Synoptic, Dynamic and General Circulation Aspect*, NASA Ref. Publ. 1017, Suitland, Md.
Mitchell, D. M., L. G. Gray, J. Anstey, M. P. Baldwin, and A. J. Charlton-Perez (2012), The influence of stratospheric vortex displacements and splits on surface climate, *J. Clim.*, *26*, 2668–2682, doi:10.1175/JCLI-D-12-00030.1.
Newman, P. A., and E. R. Nash (2000), Quantifying the wave driving of the stratosphere, *J. Geophys. Res.*, *105*(D10), 12,485–12,497, doi:10.1029/1999JD901191.
Newman, P. A., and J. E. Rosenfield (1997), Stratospheric thermal damping times, *Geophys. Res. Lett.*, *24*, 433–436.
Newman, P. A., E. R. Nash, and J. E. Rosenfield (2001), What controls the temperature of the arctic stratosphere during the spring?, *J. Geophys. Res.*, *106*, 19,999–20,010.
Palmeiro, F., D. Barriopedro, R. García-Herrera, and N. Calvo (2015), Comparing sudden stratospheric warming definitions in reanalysis data, *J. Clim.*, *28*(17), 6823–6840, doi:10.1175/JCLI-D-15-0004.1.
Pawson, S., and T. Kubitz (1996), Climatology of planetary waves in the northern stratosphere, *J. Geophys. Res.*, *101*, 16,987–16,996.
Pawson, S., and B. Naukojat (1999), The cold winters of the middle 1990s in the northern lower stratosphere, *J. Geophys. Res.*, *104*, 14,209–14,222.
Perlwitz, J., and N. Harnik (2003), Observational evidence of a stratospheric influence on the troposphere by planetary wave reflection, *J. Clim.*, *16*, 3011–3026.
Polvani, L. M, and D. W. Waugh (2004), Upward wave activity flux as a precursor to extreme stratospheric events and subsequent anomalous surface weather regimes, *J. Clim.*, *17*, 3548–3554.
Scherhag, R. (1952), Die explosionsartigen stratospherener warmungen des spatwinters 1951/52, *Ber. Deut. Wetterdienstes*, *38*, 51–63.
Stephenson, D. B., H. F. Diaz, R. J. Murnane (2008), Definition, diagnosis and origin of extreme weather and climate 43 events, in *Climate Extremes and Society*, vol. 44, edited by R. J. Murnane and H. F. Diaz, pp. 11–23, Cambridge Univ. Press, New York.
Sun, L., and W. A. Robinson (2009), Downward influence of stratospheric final warming events in an idealized model, *Geophys. Res. Lett.*, *36*, L03819, doi:10.1029/2008GL036624.
Uppala, S. M., et al. (2005), The ERA-40 re-analysis, *Q. J. R. Meteorol. Soc.*, *131*, 2961–3012, doi:10.1256/qj.04.176.
Zhou, S., A. J. Miller, J. Wang, and J. K. Angell (2002), Downward-propagating temperature anomalies in the preconditioned polar stratosphere, *J. Clim.*, *15*, 781–792, doi:10.1175/1520-0442.